Wenle Weng, Philip S. Light and Andre N. Luiten
Ultra-sensitive lithium niobate thermometer based on a dual-resonant whispering-gallery-mode cavity
Optics Letters, 2018; 43(7):1415-1418

Published version: http://dx.doi.org/10.1364/OL.43.001415

Ultra-sensitive lithium niobate thermometer based on a dual-resonant whispering-gallery-mode cavity

WENLE WENG[1,2,*], PHILIP S. LIGHT[1], AND ANDRE N. LUITEN[1,3]

[1] Institute for Photonics and Advanced Sensing and School of Physical Sciences, University of Adelaide, SA 5005, Australia
[2] currently at École Polytechnique Fédérale de Lausanne (EPFL), CH-1015 Lausanne, Switzerland
[3] e-mail: andre.luiten@adelaide.edu.au
[*] Corresponding author: wenle.weng@epfl.ch

Compiled February 1, 2018

Optical whispering-gallery-mode resonators (WGMRs) with millimeter- and micro-scales possess high quality-factors (Qs), have small footprints, and are easy to fabricate. This makes them potentially excellent candidates for compact optical frequency references [1, 2], narrow-linewidth lasers [3, 4] and frequency comb sources [5]. However, when compared with conventional Fabry-Perot optical cavities [6–8], WGMRs confine the majority of the electromagnetic field energy inside a dielectric material. This introduces a high sensitivity of the mode frequencies to technical and fundamental temperature fluctuations because of a direct sensitivity to thermal expansion and thermooptic effects. A number of dual-mode, self-referenced techniques have been developed to overcome these shortcomings by sensing the temperature fluctuations and subsequently stabilizing the temperature [2, 9–12]. Although the detailed implementations vary, the underlying principle is always the same: one exploits the polarization or wavelength dependence of the thermooptic coefficients to measure the resonator temperature through the frequency difference of two modes. This yields an in-situ measure of the resonator temperature which can thus be controlled.

Temperature sensitivity is one of the most important figures of merit for characterizing the thermometer performance. With the same noise floor the detection limit is inversely proportional to the sensitivity, therefore a large sensitivity allows for better resolution of thermometry. While extremely high sensitivities have been demonstrated in a variety of optical thermometers [13–17], the previously reported sensitivities of CaF_2 and MgF_2 WGMR-based dual-mode thermometers only reached $\sim 80 - 500$ MHz/K [9–11]. In this work, we use a millimeter-size lithium niobate (LN) WGMR as the birefringent resonator in a dual-polarization thermometry technique. The large difference in the thermooptic coefficients of orthogonal polarizations yields an unprecedented temperature sensitivity of 3.0 GHz/K. In order to precisely measure the frequency difference between two resonant modes so to achieve a low noise floor, we adopt an intracavity modulation technique that allows us to implement a Pound-Drever-Hall (PDH) laser locking technique [18] without the need for any auxiliary frequency modulation technique. Using the fluctuation-dissipation theorem (FDT) we calculate the fundamental thermal noise of the resonator, showing that the performance of this thermometer could be improved by up to another factor of 10 with better frequency locking.

Fig. 1 shows the scheme of the dual-resonance thermometer. The LN WGMR has a diameter of 9.5mm with a thickness of 1mm and is fabricated from a z-cut crystalline substrate using the surface polishing technique [19]. The light from two 1560 nm lasers (Laser 1 and Laser 2) are transferred by polarization-maintaining fiber and then coupled into two modes with orthogonal polarizations via a rutile prism. The polarization of the two laser signals is adjusted so that Laser 1 is coupled into a TM mode, while Laser 2 is coupled into a TE mode. Both laser signals pass through acousto-optic modulators (AOMs) that allow for rapid frequency corrections so that the laser frequencies can be tightly locked to their respective modes. Due to the birefringence of the LN resonator and the prism, there is a $\sim 50^\circ$ difference in the in-plane incident angles for optimal in and out coupling of the two laser beams. This fortunate arrangement means that it is not necessary to use polarizing components on either the input or output coupling to the resonator - the spatial separation alone is sufficient to let the two beams be separately registered on two independent photodetectors. The resonator exhibits a nearly identical loaded Q of $\sim 1.3 \times 10^8$ for both polarizations, which corresponds to a bandwidth of 1.5 MHz. In the following experiment we have adjusted the coupling to keep the resonator as close as possible to the critical coupling condition. This shows a coupling efficiency of around $\sim 40\%$ due to imperfect spatial mode matching at the prism. To avoid any distortion of mode spectrum through thermal nonlinearity we couple only ~ 200 nW of laser power into the resonator. With such relatively small couple-in power, the Kerr noise and the temperature noise produced by the laser RIN, which is below -90 dBc/Hz at 1 Hz and below -130 dB/Hz at frequency range above 100 Hz, is much lower than the laser locking noise [1, 11].

The conventional approach to lock the frequency of a laser to a mode of a resonator is to use the PDH technique in which the incident laser light is phase modulated. Synchronous detection of the reflected light field provides a dispersive-like signal that can be used to steer the laser frequency to the resonance. In this experiment we have taken the inverse approach and modulated the resonant cavity while leaving the incident laser signal untouched. This leads to a simpler arrangement in which no external modulator is required and also leads to very good performance. We apply a 4 MHz z-directed electric field across the resonator using electrodes on the top and bottom faces. This

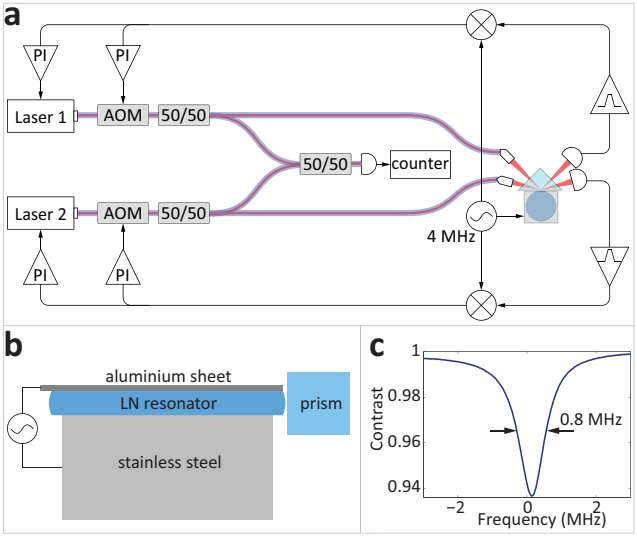

Fig. 1. A schematic of the experimental setup. (a) Two 1560 nm lasers are frequency-locked to two modes of orthogonal polarizations respectively. A 4 MHz signal from a function generator is applied to the resonator to create frequency-modulated modes, which are used to generate PDH error signals (see text for details). These signals are then used to lock the laser frequencies to the modes. A dead-time-free counter is used to measure the difference frequency between the two lasers.(b) Electrooptic modulation setup. A piece of thin aluminum sheet was clamped to be in good contact with the top surface of the resonator. A peak-to-peak voltage of ~ 0.5 V is ap-plied to the resonator along z-axis with frequency of 4 MHz to carry out the frequency modulation for PDH laser locking.(c) A mode spectrum shows an undercoupled bandwidth of 0.8 MHz.

generates frequency modulation of the resonant modes with a modulation index of around 0.7. Similar to the conventional PDH technique, the incident light interacts with the frequency-modulated mode to generate an amplitude-modulation (AM) signal whose magnitude depends on the difference frequency between the laser and the average mode frequency. The signals out of each of the photodetectors is separately demodulated at the 4 MHz modulation frequency to generate an error signal to lock each of the two lasers. Fast frequency fluctuations are corrected by modulating the driving frequency of the AOMs at the outputs of the lasers, while slower fluctuations are corrected by using the error signals to directly modulate the laser frequency itself. This scheme could be further simplified by using just one laser source and single AOM [11]. The difference frequency between the two resonant modes is obtained by combining the light from the two lasers using fiber-coupled splitters and then sending these signals to a fast photodetector. The difference frequency is recorded by a dead-time-free counter.

The temperature dependence of the frequency of a resonant mode in a birefringent resonator can be expressed as:

$$\frac{df_{\mathrm{TE(TM)}}}{dT} = -f_{\mathrm{TE(TM)}}\left(\alpha + \frac{\beta_{\mathrm{o(e)}}}{n_{\mathrm{o(e)}}}\right) \quad \textbf{(1)}$$

where $f_{\mathrm{TE(TM)}}$ is the resonance frequency of a mode of TE (TM) polarization, $n_{\mathrm{o(e)}}$ is the ordinary (extraordinary) refractive index, $\beta_{\mathrm{o(e)}}$ is the thermooptic coefficient which corresponds to the TE (TM) light whose polarization is parallel (perpendicular) to the optical axis of the resonator, and α is the thermal expansion coefficient. For LN at room temperature $\alpha = 1.35 \times 10^{-5}\,\mathrm{K}^{-1}$ is used for the linear thermal expansion coefficient along the direction perpendicular to the optical axis [20] due to the fact that it is the resonator edge displacement along the radial direction that contributes to the resonance frequency shift through thermal expansion. In this case it follows that the temperature dependence of the frequency difference between two orthogonally polarized modes is:

$$\frac{df_{\mathrm{diff}}}{dT} \approx -f_{\mathrm{laser}}\left(\frac{\beta_{\mathrm{e}}}{n_{\mathrm{e}}} - \frac{\beta_{\mathrm{o}}}{n_{\mathrm{o}}}\right) \quad \textbf{(2)}$$

We calculate the refractive indices of LN at wavelength of 1.56 μm according to Sellmeier equations and derive $n_{\mathrm{o}} = 2.21$ and $n_{\mathrm{e}} = 2.14$ [21]. The thermooptic coefficients of LN have been given as $\beta_{\mathrm{o}} = 0\,\mathrm{K}^{-1}$ and $\beta_{\mathrm{e}} = 3.34 \times 10^{-5}\,\mathrm{K}^{-1}$ at 1523 nm [22]. With these parameters, we predict a temperature sensitivity of the TM mode as $\frac{df_{\mathrm{TM}}}{dT} = 5.6\,\mathrm{GHz/K}$, while the difference frequency between the two orthogonal modes as $\frac{df_{\mathrm{diff}}}{dT} = 3.0\,\mathrm{GHz/K}$.

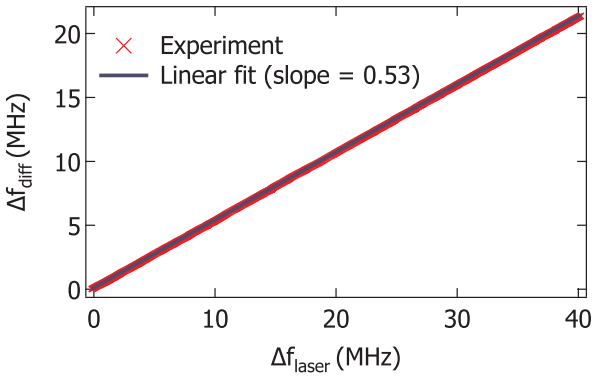

Fig. 2. Relation between Δf_{diff} and $\Delta f_{\mathrm{Laser}}$ while the resonator temperature drifts. A linear relation of $\Delta f_{\mathrm{diff}} = 0.53 \times \Delta f_{\mathrm{laser}}$ is revealed with fitting of the experimental data.

These expectations can be tested by measuring Δf_{TM} and Δf_{diff} as the temperature of the thermometer is varied. The frequency variations of Laser 1 ($\Delta f_{\mathrm{laser}}$) are measured by comparing to an auxiliary 1560 nm laser that is frequency locked to an ultrastable cavity with relative frequency instability of $< 1 \times 10^{-14}$ at 1 s integration time. We simultaneously record over a few minutes $\Delta f_{\mathrm{laser}}$ and Δf_{diff} as the resonator temperature varies due to ambient temperature drift. We plot the resulting Δf_{diff} against $\Delta f_{\mathrm{laser}}$ on Fig. 2 along with a linear fit of the data. We find a relation of $\Delta f_{\mathrm{diff}} = 0.53 \times \Delta f_{\mathrm{laser}}$, showing excellent agreement with our prediction ($\Delta f_{\mathrm{diff}} = 0.54 \times \Delta f_{\mathrm{laser}}$).

This experiment confirms a thermometer sensitivity of $\frac{df_{\mathrm{diff}}}{dT} = 3.0\,\mathrm{GHz/K}$, which is, to our knowledge, the highest sensitivity of dual-mode thermometer ever reported and more than an order of magnitude larger than that of MgF_2-based thermometers. We note that there has been some recent work on dual-resonant thermometry in LN microdisks [23]. In that case a temperature sensitivity of 0.834 GHz/K is reported due to a significant portion of the electromagnetic energy being in the evanescent field outside the dielectric. In contrast, the millimeter-size WGMRs reported here confines almost all light energy within the host material, resulting in the full exploitation of the large thermooptic coefficient difference.

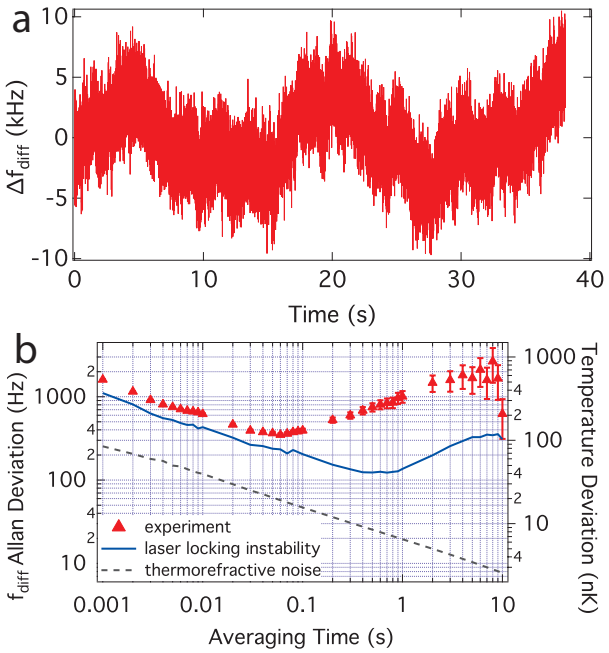

Fig. 3. (a) Frequency fluctuations of f_{diff} measured with frequency counting of the beat frequency. (b) Allan deviation comparison of the measured frequency fluctuations of f_{diff} and the projected temperature fluctuations. Independently measured laser locking instability of the system is plotted in blue. Dashed grey trace shows the fundamental thermorefractive noise of the thermometer.

In Fig. 3 (a) we present the fluctuations of f_{diff} over 40 seconds with a counting rate of 1 kHz. We have subtracted a linear drift from this data to make the fluctuations easier to visualise. In Fig. 3 (b) we display the Allan frequency deviations of these frequency measurements as well as the corresponding temperature fluctuations using our earlier calibration. We have independently measured the residual noise of the laser frequency locking and display this in terms of the corresponding Allan frequency deviations on Fig. 3 (b). We observe that the fluctuations of f_{diff} for averaging times longer than 0.1 s are significantly higher than the laser locking instabilities – these are consistent with flicker noise that arises from environmental temperature fluctuations as well as laser power fluctuations.

In addition to the technical laser locking limits one should consider any fundamental noises that will limit the thermometry performance. Thermorefractive fluctuations turn out to be the dominant noise source because of the small effective mode volume and the large thermooptic coefficient in crystalline WGMRs [24, 25]. And because the thermooptic coefficient of TE mode vanishes in our work, only the thermorefractive noise of the TM mode needs to be considered. In earlier works thermorefractive noise was investigated analytically with Langevin's method [25, 26]. However, this method is mathematically tedious, particularly when one attempts to undertake more sophisticated thermal models that include multiple pathways for thermal connection between the resonator and the environment (e.g. taking into account the post attached to the WGMR). Here we use simulations based on FDT [27, 28] to calculate the thermorefractive noise with finite-element method (FEM) based on dynamics of heat transfer [29–31]. Fig. 4 (a) shows the geometry of the model. The stainless steel post is included in our model as a channel for thermal energy dissipation. In principle, it is possible to include additional thermal channels such as thermal transport though the surrounding air to yield better estimation of thermal noise at low frequency. However for the frequency range considered here we did not need to consider these additional couplings.

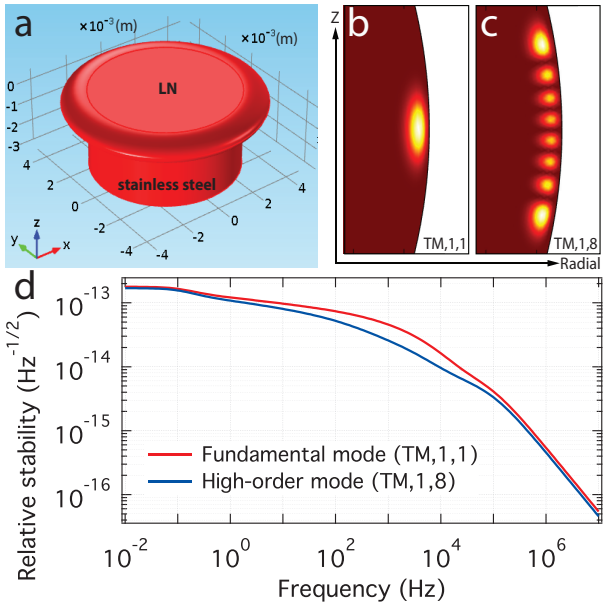

Fig. 4. (a) Geometry of the FEM model for calculating fundamental thermal noise based on FDT. (b, c) Heat source profiles for a fundamental mode and a high order mode respectively. The size of each figure is 100 μm (height)$\times$50 μm (width). (d) Thermorefractive noise spectra of the two modes.

The model heat source corresponds to the intensity profile of the optical mode and this is calculated with quasi-2D-FEM method [32]. Following this we solve the heat transfer in 2D-axisymmetric fashion. In each case we calculate the dissipated power using varying modulation frequencies for the heat source power. Using this approach we calculate the thermorefractive noise of a fundamental TM mode (denoted as *TM,1,1* in Fig. 4). In the same figure we also present the noise spectrum of a high-order TM mode (*TM,1,8*) for comparison. Such high order mode possesses a larger mode volume as well as a very different intensity distribution to the fundamental mode. We also found that we could efficiently couple light into this mode in the experiment, which potentially allows us to test the quality of our simulation. Fig. 4 (b) and (c) show the heat source profiles of the two modes respectively in false color. In Fig. 4 (d) are the noise spectra of the two modes. The fundamental mode exhibits a slightly higher noise level because of smaller effective mode volume. We translate the noise spectrum of the fundamental mode into an Allan frequency deviations and have plotted these also on Fig. 3 (b) (dashed line). With this simulation we show that the fundamental noise of the thermometer is a factor of ~ 5 lower than the laser locking instabilities for averaging times of 0.001–1 s. This opens the door to a thermometer with a detectivity of a few nK at averaging time of 1 s. In order to improve the locking performance one could use a pre-stabilized laser with better noise performance than the one used here along with better residual amplitude noise suppression to improve the long-term performance[33–35].

In conclusion, we have demonstrated a dual-resonant ther-

mometer based on a LN WGMR with an unprecedented temperature sensitivity of 3.0 GHz/K owing to the large difference in thermooptic coefficients of orthogonal polarizations in LN. We perform PDH laser locking using an intracavity phase modulation technique. Such a technique removes the requirement of an extra phase modulation component such as an EOM or AOM, thus facilitating the application and packaging of the thermometer. It should be noted that with engineering of the resonator geometry and the electrodes the sensitivity of the thermometer could be enhanced by the pyroelectric effect [16] as has been recently observed in LN WGMRs [36]. With this enhanced sensitivity and improved laser locking stability it would suggest that the fundamental-thermal-noise-limited-detectivity may be reached.

ACKNOWLEDGEMENT

We are grateful to Bruce Candy for providing low noise photodetectors. W. W. thanks D. Heinert for help with the FEM simulation. We also wish to thank the referees for bringing to our attention the potential benefits of pyroelectric effects.

FUNDING INFORMATION

Australian Research Council (ARC) (DP0877938, FT0991631, LE110100054, LE100100009); South Australian Government Premier's Science and Research Fund.

REFERENCES

1. J. Alnis, A. Schliesser, C. Y. Wang, J. Hofer, T. J. Kippenberg, and T. W. Hänsch, "Thermal-noise-limited crystalline whispering-gallery-mode resonator for laser stabilization," Phys. Rev. A **84**, 011804 (2011).
2. L. M. Baumgartel, R. J. Thompson, and N. Yu, "Frequency stability of a dual-mode whispering gallery mode optical reference cavity," Optics Express **20**, 29798–29806 (2012).
3. B. Sprenger, H. Schwefel, Z. Lu, S. Svitlov, and L. Wang, "Caf< sub> 2</sub> whispering-gallery-mode-resonator stabilized-narrow-linewidth laser," Opt. Lett. **35**, 2870–2872 (2010).
4. W. Liang, V. Ilchenko, A. Savchenkov, A. Matsko, D. Seidel, and L. Maleki, "Whispering-gallery-mode-resonator-based ultranarrow linewidth external-cavity semiconductor laser," Opt. Lett. **35**, 2822–2824 (2010).
5. T. J. Kippenberg, R. Holzwarth, and S. Diddams, "Microresonator-based optical frequency combs," Science **332**, 555–559 (2011).
6. J. Millo, D. V. Magalhaes, C. Mandache, Y. Le Coq, E. M. L. English, P. G. Westergaard, J. Lodewyck, S. Bize, P. Lemonde, and G. Santarelli, "Ultrastable lasers based on vibration insensitive cavities," Phys. Rev. A **79**, 053829 (2009).
7. T. Kessler, C. Hagemann, C. Grebing, T. Legero, U. Sterr, F. Riehle, M. Martin, L. Chen, and J. Ye, "A sub-40-mhz-linewidth laser based on a silicon single-crystal optical cavity," Nat. Photonics **6**, 687–692 (2012).
8. D. G. Matei, T. Legero, S. Häfner, C. Grebing, R. Weyrich, W. Zhang, L. Sonderhouse, J. M. Robinson, J. Ye, F. Riehle, and U. Sterr, "1.5 μm lasers with sub-10 mhz linewidth," Phys. Rev. Lett. **118**, 263202 (2017).
9. D. V. Strekalov, R. J. Thompson, L. M. Baumgartel, I. S. Grudinin, and N. Yu, "Temperature measurement and stabilization in a birefringent whispering gallery mode resonator," Opt. Express **19**, 14495–14501 (2011).
10. I. Fescenko, J. Alnis, A. Schliesser, C. Wang, T. Kippenberg, and T. Hänsch, "Dual-mode temperature compensation technique for laser stabilization to a crystalline whispering gallery mode resonator," Opt. Express **20**, 19185–19193 (2012).
11. W. Weng, J. D. Anstie, T. M. Stace, G. Campbell, F. N. Baynes, and A. N. Luiten, "Nano-kelvin thermometry and temperature control: beyond the thermal noise limit," Physical review letters **112**, 160801 (2014).
12. S. Tan, S. Wang, S. Saraf, and J. A. Lipa, "Pico-kelvin thermometry and temperature stabilization using a resonant optical cavity," Optics Express **25**, 3578–3593 (2017).
13. M. Chomat, J. Čtyrokỳ, D. Berková, V. Matějec, J. Kaňka, J. Skokankova, F. Todorov, A. Jančárek, and P. Bittner, "Temperature sensitivity of long-period gratings inscribed with a co2 laser in optical fiber with graded-index cladding," Sensors and Actuators B: Chemical **119**, 642–650 (2006).
14. Y. Liu, B. Liu, X. Feng, W. Zhang, G. Zhou, S. Yuan, G. Kai, and X. Dong, "High-birefringence fiber loop mirrors and their applications as sensors," Applied optics **44**, 2382–2390 (2005).
15. W. Qian, C.-L. Zhao, S. He, X. Dong, S. Zhang, Z. Zhang, S. Jin, J. Guo, and H. Wei, "High-sensitivity temperature sensor based on an alcohol-filled photonic crystal fiber loop mirror," Optics letters **36**, 1548–1550 (2011).
16. H. Lu, B. Sadani, G. Ulliac, C. Guyot, N. Courjal, M. Collet, F. I. Baida, and M.-P. Bernal, "Integrated temperature sensor based on an enhanced pyroelectric photonic crystal," Optics Express **21**, 16311–16318 (2013).
17. W. Qiu, A. Ndao, V. C. Vila, R. Salut, N. Courjal, F. I. Baida, and M.-P. Bernal, "Fano resonance-based highly sensitive, compact temperature sensor on thin film lithium niobate," Optics letters **41**, 1106–1109 (2016).
18. E. D. Black, "An introduction to pound–drever–hall laser frequency stabilization," American Journal of Physics **69**, 79–87 (2001).
19. I. S. Grudinin, A. B. Matsko, A. A. Savchenkov, D. Strekalov, V. S. Ilchenko, and L. Maleki, "Ultra high q crystalline microcavities," Optics Communications **265**, 33–38 (2006).
20. F. Pignatiello, M. De Rosa, P. Ferraro, S. Grilli, P. De Natale, A. Arie, and S. De Nicola, "Measurement of the thermal expansion coefficients of ferroelectric crystals by a moiré interferometer," Optics communications **277**, 14–18 (2007).
21. D. E. Zelmon, D. L. Small, and D. Jundt, "Infrared corrected sellmeier coefficients for congruently grown lithium niobate and 5 mol.% magnesium oxide–doped lithium niobate," JOSA B **14**, 3319–3322 (1997).
22. L. Moretti, M. Iodice, F. G. Della Corte, and I. Rendina, "Temperature dependence of the thermo-optic coefficient of lithium niobate, from 300 to 515 k in the visible and infrared regions," (2005).
23. R. Luo, H. Jiang, H. Liang, Y. Chen, and Q. Lin, "Self-referenced temperature sensing with a lithium niobate microdisk resonator," Optics Letters **42**, 1281–1284 (2017).
24. M. L. Gorodetsky and I. S. Grudinin, "Fundamental thermal fluctuations in microspheres," J. Opt. Soc. Am. B **21**, 697–705 (2004).
25. A. B. Matsko, A. A. Savchenkov, N. Yu, and L. Maleki, "Whispering-gallery-mode resonators as frequency references. i. fundamental limitations," J. Opt. Soc. Am. B **24**, 1324–1335 (2007).
26. V. Braginsky, M. Gorodetsky, and S. Vyatchanin, "Thermodynamical fluctuations and photo-thermal shot noise in gravitational wave antennae," Physics Letters A **264**, 1 – 10 (1999).
27. Y. Levin, "Fluctuation–dissipation theorem for thermo-refractive noise," Physics Letters A **372**, 1941–1944 (2008).
28. B. Benthem and Y. Levin, "Thermorefractive and thermochemical noise in the beamsplitter of the geo600 gravitational-wave interferometer," Physical Review D **80**, 062004 (2009).
29. D. Heinert, A. Gurkovsky, R. Nawrodt, S. Vyatchanin, and K. Yamamoto, "Thermorefractive noise of finite-sized cylindrical test masses," Physical Review D **84**, 062001 (2011).
30. D. Heinert, G. Hofmann, and R. Nawrodt, "Fluctuation dissipation at work: Thermal noise in reflective optical coatings for gw detectors," in "Metrology for Aerospace (MetroAeroSpace), 2014 IEEE," (IEEE, 2014), pp. 293–298.
31. N. Kondratiev and M. Gorodetsky, "Thermorefractive noise in whispering gallery mode microresonators: Analytical results and numerical simulation," Physics Letters A (2017).
32. M. Oxborrow, "Traceable 2-d finite-element simulation of the whispering-gallery modes of axisymmetric electromagnetic resonators," Microwave Theory and Techniques, IEEE Transactions on **55**, 1209–1218 (2007).
33. F. du Burck, O. Lopez, and A. El Basri, "Narrow-band correction of the

residual amplitude modulation in frequency-modulation spectroscopy," IEEE Transactions on Instrumentation and Measurement **52**, 288–291 (2003).
34. W. Zhang, M. Martin, C. Benko, J. Hall, J. Ye, C. Hagemann, T. Legero, U. Sterr, F. Riehle, G. Cole *et al.*, "Reduction of residual amplitude modulation to $1\times$ 10-6 for frequency modulation and laser stabilization," Optics letters **39**, 1980–1983 (2014).
35. Z. Tai, L. Yan, Y. Zhang, X. Zhang, W. Guo, S. Zhang, and H. Jiang, "Electro-optic modulator with ultra-low residual amplitude modulation for frequency modulation and laser stabilization," Optics letters **41**, 5584–5587 (2016).
36. M. Leidinger, C. S. Werner, W. Yoshiki, K. Buse, and I. Breunig, "Impact of the photorefractive and pyroelectric-electro-optic effect in lithium niobate on whispering-gallery modes," Optics letters **41**, 5474–5477 (2016).